Investigation of a 600-GHz Membrane-Based Twin Slot Antenna for HEB Mixers

W. Miao[1, 2,*], Y. Delorme[1], F. Dauplay[1], R. Lefevre[1], B. Lecomte[1], A. Feret[1], G. Beaudin[1], J. M. Krieg[1], W. Zhang[2], S. H. Cheng[2], and S. C. Shi[2].

[1]LERMA, Observatoire de Pairs, France
[2]Purple Mountain Observatory, NAOC, CAS, China
* Contact: wei.miao@obspm.fr, phone: 33-1-40-51-20-60

***Abstract*—In this paper, a 600-GHz membrane-based twin slot antenna for superconducting HEB (hot-electron-bolometer) mixers was investigated. The simulation on the radiation pattern and return loss (refer to the feed point) of the twin slot antenna including an RF choker filter was performed with Microwave Studio CST, Ansoft HFSS, and EMSS FEKO. An additional parabolic mirror is taken into account as focusing element in the membrane-based design and analyzed by using physical optics ray tracing approximation. We also fabricated a 200-times scale model of the designed twin slot antenna to validate the simulated results. For the scale model measurement, a de-embedding measurement technique was adopted to extract the input impedance of the twin slot antenna. The measured results are found in good agreement with the simulation.**

I. INTRODUCTION

FOR development of a closely packed multi-pixel superconducting HEB receiver, a new integrated quasi-optical design was proposed [1] to achieve efficient RF radiation coupling. The planar quasi-optical antenna in this design is integrated on an electrically thin substrate (membrane) and it couples the RF radiation via a metallic back reflector and a parabolic mirror (as shown in Fig. 1). Normally, the thickness of the membrane is less than 0.04 λ_0 (for slot antenna) [2] to avoid excitation of substrate modes. In contrast with the conventional substrate-lens integrated configuration, the absence of a thick substrate reduces the dielectric loss and enlarges the antenna structure. The usage of an antenna with a large dimension makes the device fabrication process much easier, especially for very high frequencies like terahertz. In this paper, we thoroughly investigate the quasi-optical properties of this new design incorporating with a planar twin slot antenna. At 600-GHz the radiation pattern and return loss of a membrane-based twin slot antenna were simulated with the aid of three different full wave electromagnetic solvers. The simulated input impedance (i.e. feed point impedance) of the twin slot antenna is validated by a 200-times scale model measurement employing a de-embedding technique.

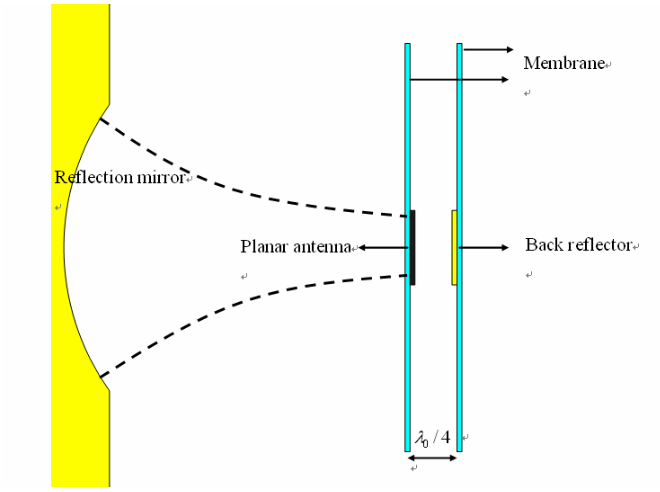

Fig. 1. Configuration of a membrane based quasi optical antenna.

II. NUMERICAL SIMULATION

A. Design of a Membrane-Based Twin Slot Antenna

Planar twin slot antennas have been widely used in quasi-optical receivers to achieve highly symmetric Gaussian beams and low cross polarization levels. The conventional design rule for twin slot antennas based on a scale model [3], is no longer valid for membrane-based twin slot antennas since the membrane is extremely thin and the substrate's influence is no longer same [1]. Therefore we defined the membrane-based twin slot antenna with the aid of a full wave electromagnetic solver Microwave Studio CST [4], which is based on the method of finite integration technique. Fig. 2 illustrates the simulated structure by Microwave Studio CST. The twin slot antenna is integrated on the membrane and a metallic back reflector is placed at a quarter-wavelength (in vacuum) behind the antenna for increasing the antenna's gain. The membrane is made of a silicon-on-insulator (SOI) wafer with a thickness of 3 μm and a dielectric constant of 11.7. An RF choker filter consisting of three consecutive low and high impedance quarter wavelength CPW stages is included to prevent the leakage of the RF signal into the IF port without stopping the IF and DC signal.

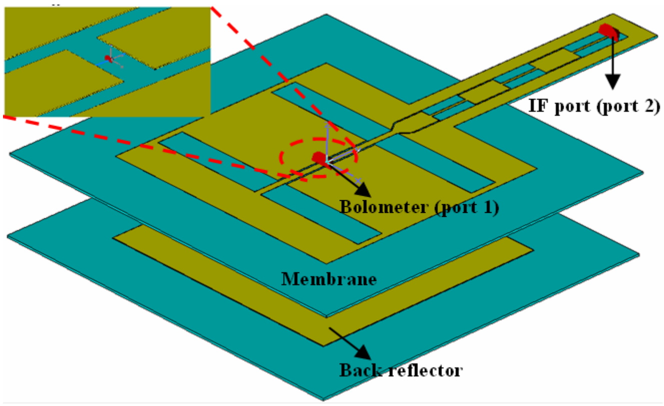

Fig. 2. CST simulated structure of the twin slot antenna. The bolometer (discrete port) is located on the center and coupled with the twin slot antenna via CPW lines.

In the simulation, the bolometer (i.e. HEB) is taken as a discrete port, designated as port 1, with a reference impedance of 100 Ω and coupled with the twin slot antenna via coplanar waveguide (CPW) transmission lines. The IF port, at the end of the RF choker filter, is defined as the other discrete port (port 2) with a reference impedance of 50 Ω. The reference impedance of port 1 was chosen to be analogous to the normal-state impedance (normally around 100 Ω) of our superconducting HEB devices. Fig. 3 shows the simulated reflection and transmission coefficients of this two-port network after optimizing the antenna's parameters for the minimum return loss at the antenna's feed point at 600 GHz. The optimized length and width of the slot is 350 μm (0.7 λ_0) and 43.5 μm (0.087 λ_0) respectively. According to Fig. 3, we can find that the twin slot antenna is well matched (to 100 Ω) at the design frequency of 600 GHz with a 10% relative bandwidth at a return-loss ($|S_{11}|^2$) level below -20 dB. The reflection coefficient at IF port is nearly equal to 0 dB, indicating that the field transmission between the two ports is efficiently prevented by the RF choker filter in the design frequency range. The superposition of the transmission coefficients (S_{12} and S_{21}) indicates the reciprocity of this two-port network and makes possible the application of the de-embedding technique between two ports. Fig. 4 shows the simulated radiation patterns of the twin slot antenna. Nearly perfectly symmetric radiation patterns are obtained in both E- and H-plane within a large angle range (100 degree). Notice that the effect of the parabolic mirror is not taken into account for the moment due to its extremely large size.

B. Comparison with HFSS and FEKO

In order to validate the optimized results, we simulated the same structure of the membrane-based twin slot antenna with two other full wave electromagnetic solvers Ansoft HFSS [5] and EMSS FEKO [6] based respectively on finite element method (FEM) and on method of moment (MoM). Fig. 3 and Fig. 4 show the simulated results with respect to return loss and radiation pattern. Clearly these three electromagnetic solvers have given nearly identical results over the whole frequency

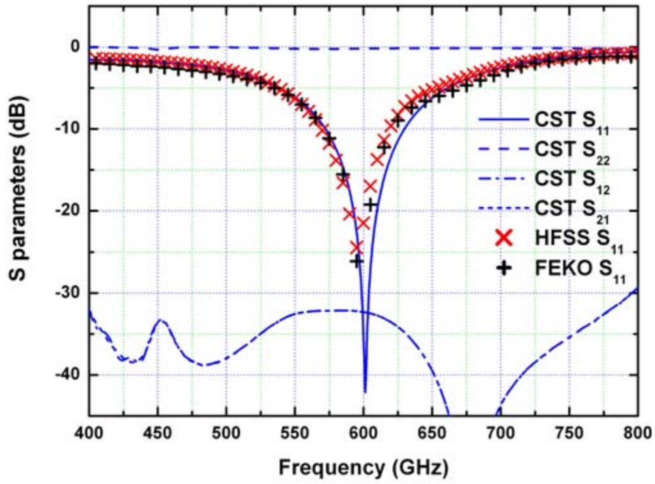

Fig. 3. Simulated *S* parameters seen from bolometer and IF port as a function of frequency.

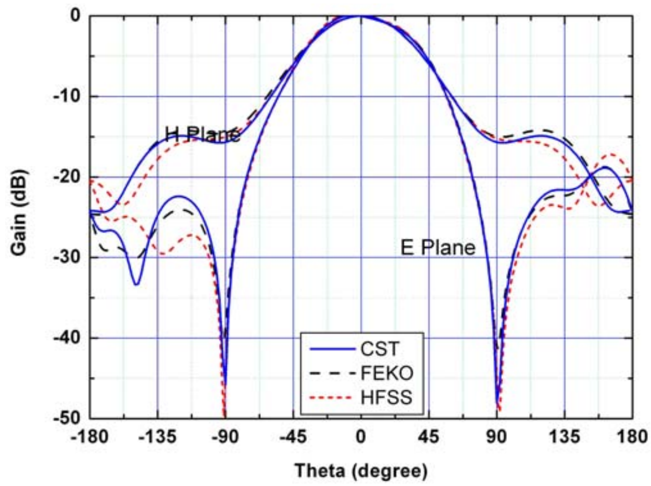

Fig. 4. Radiation patterns of the membrane-based twin slot antenna.

range. The insignificant frequency shift (Fig. 3) may be caused by the different mesh definition around the feed port

(port 1) which is extremely small in comparison to the twin slot antenna.

C. Effect of a parabolic mirror

We evaluated the effect of a parabolic mirror to the integrated antenna by means of an asymptotic high frequency technique employing physical optics (PO) ray tracing approximation. This technique has been hybridized by EMSS FEKO to solve electromagnetic problems when the object under consideration is too large (in terms of wavelength) to be dealt with by MoM.

The parabolic mirror adopted in our analysis has a diameter of 5 mm and a focal length of 2.5 mm. The membrane-based twin slot antenna is placed on the focal plane of the mirror and firstly simulated by using MoM. The results are then used as an input for the physical optics (PO) ray tracing approximation to simulate the whole mirror-membrane-based antenna

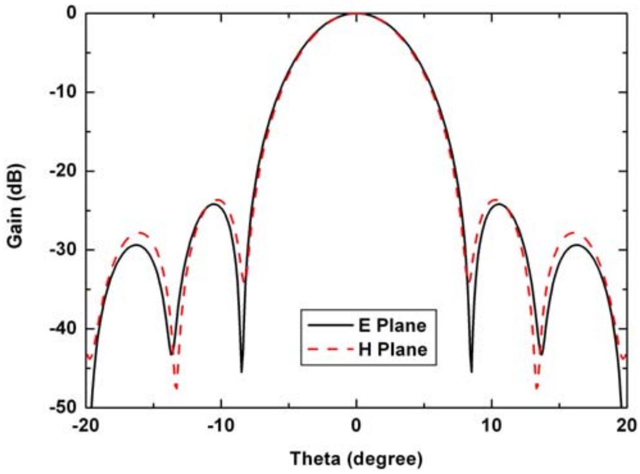

Fig. 5. Radiation patterns in E- and H-Plane of the membrane-based twin slot antenna including a 5 mm parabolic mirror.

structure. The calculated radiation patterns in E- and H-Plane at 600 GHz are illustrated in Fig. 5. The first side lobe level in two planes drops to -24 dB and the HPBW (Half Power Beam Width) of main lobe is around 6.4°, while 5.9° was given by diffraction limited beam pattern calculated [7] by the expression $(2J_1(\nu)/\nu)^2$, where $\nu = (\pi \tan(\theta) D)/\lambda_0$, J_1 is the first-order Bessel function of the first kind and D is the diameter of the mirror. It suggests that a diffraction-limited beam pattern can be achieved with the proposed quasi-optical design combining membrane-based twin slot antenna with parabolic mirror.

III. Scale Model Measurement

We also fabricated a 200 times scale model, as shown in Fig. 6, for the membrane-based twin slot antenna to validate the simulated results. In this model, the SOI membrane was replaced by a 0.635 mm thick high frequency laminate RT/Duroid 6006/6010 (ε_r = 10.8±0.25) [8]. As superconducting HEB devices can be equivalent to a resistance, we adopted a three-standard de-embedding measurement technique [9], [10] to characterize the input impedance of the twin slot antenna. Notice that in order to avoid too small (e.g. smaller than -20 dB) reflection coefficients measured at the IF port for the three standards, which may affect the accuracy of the de-embedding measurement technique, here we removed the RF choke filter and preserved only the tapered section used to connect the RF choke filter and the CPW.

This de-embedding measurement technique extracts the scattering parameters of the twin slot antenna from the reflection coefficients measured at the IF port when the feed point of the twin slot antenna is terminated with three different impedance standards. In terms of the extracted scattering parameter S_{11}, the input impedance of the twin slot antenna can

Fig. 6. Left: photo of a 200 times scale model fabricated for the membrane-based twin slot antenna and Right: experimental setup used to measure the impedance of a chip resistor.

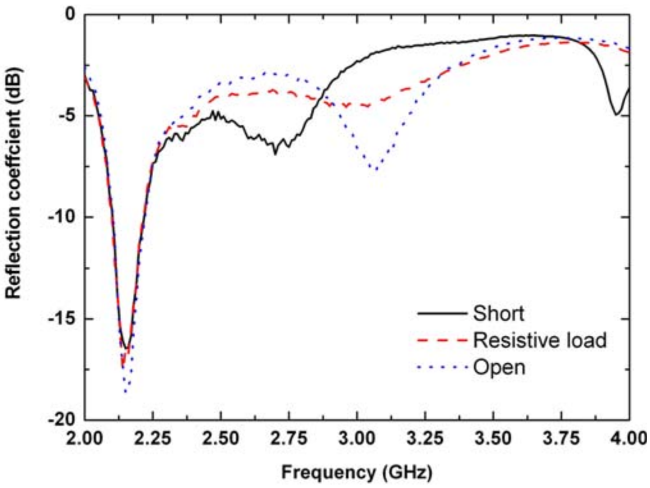

Fig. 7. Reflection coefficients measured at the IF port for three respective standards (open, short, resistive load) terminated at the feed point of the twin slot antenna.

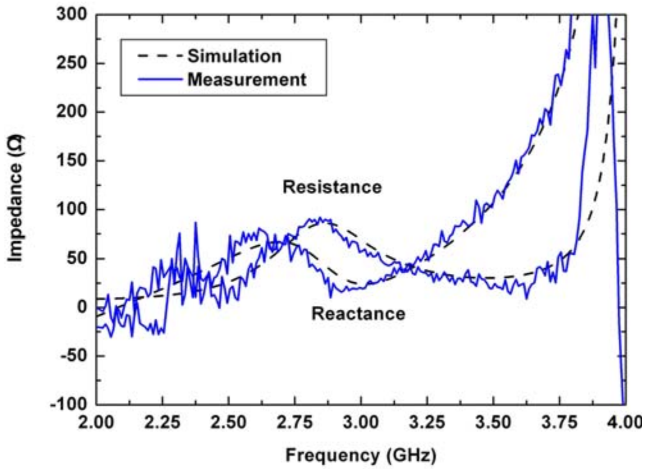

Fig. 8. Input impedances calculated by Microwave Studio CST and extracted from the scale model measurement.

be calculated by

$$Z_{input} = Z_0 \frac{1+S_{11}}{1-S_{11}} = \frac{\Gamma_1 Z_{L1}(Z_{L3}-Z_{L2}) + \Gamma_2 Z_{L2}(Z_{L1}-Z_{L3}) + \Gamma_3 Z_{L3}(Z_{L2}-Z_{L1})}{\Gamma_1(Z_{L2}-Z_{L3}) + \Gamma_2(Z_{L3}-Z_{L1}) + \Gamma_3(Z_{L1}-Z_{L2})} \quad (1)$$

where Z_0 is an arbitrarily specified reference impedance at port 1. Z_{Li} (i=1, 2, 3) and Γ_i (i=1, 2, 3) denote the impedance standards at the feed point of the twin slot antenna and the corresponding complex reflection coefficients measured at the IF port, respectively. For our scale model measurement, we chose open, short and resistive load as the three impedance standards. The input impedance can be therefore simplified as

$$Z_{input} = Z_r(\Gamma_o - \Gamma_r)/(\Gamma_r - \Gamma_s) \quad (2)$$

Where Γ_i (i=o, s, r) denote the reflection coefficients measured at the IF port when the feed point of the twin slot antenna is terminated by open, short and resistive load, and Z_r is the impedance of the resistive load.

According to Eq. (2), we know that having an accurate value of the resistive load is crucial to the de-embedding measurement technique. An additional experimental set, as shown in Fig. 6, was employed to determine the impedance of the chip resistor, which has a nominal resistance of 47.5 Ω. We soldered the chip resistor at the center of a microstrip line (DUT) with a width of 0.5 mm. The microstrip lines have the same substrate as that of the scale model. In order to remove the discontinuity effect between the SMA connector and the microstrip line as well as the loss and phase shift of the microstrip line, we also fabricated a corresponding microstrip calibration kit including Thru, Reflect and Line (shown in Fig. 6). After performing the standard TRL calibration, the impedance of the chip resistor was extracted from the measured *S* parameters of the DUT. It has a real part (from 48 to 56 Ω) close to its nominal value and a small imaginary component around 10 Ω.

Fig. 7 shows the reflection coefficients measured at the IF port when the feed point of the twin-slot antenna is terminated with three different standards (open, short, resistive load). Using these results and the measured load impedance Z_r, we calculated the input impedance of the twin slot antenna in terms of Eq. (2). Fig. 8 shows the calculated results. Clearly, the measured impedance agrees well with the one simulated by Microwave Studio CST in the frequency range of 2.5 to 4 GHz. A small discrepancy at low frequencies (from 2.0 to 2.4 GHz) might be caused by extremely low transmission between the two ports since the reflection coefficient measured at the IF port in this frequency range is indeed almost independent of the load terminated at the feed point of the twin-slot antenna (refer to Fig. 7).

Conclusion

A 600-GHz membrane-based twin slot antenna for superconducting HEB mixers has been investigated by numerical simulation and scale model measurement. The twin slot antenna is well resonant at the design frequency with a 10% relative bandwidth at return-loss level below -20 dB. A nearly diffraction-limited radiation pattern with a HPBW of 6.4°and a side lobe level of -24 dB is obtained after considering the effect of a 5 mm parabolic mirror. The validation of the simulated results of the membrane-based twin slot antenna is performed by a 200-times scale model incorporating with a three-standard de-embedding measurement technique. The measured results agree well with the numerical simulation.

ACKNOWLEDGMENT

W. M. would like to thank French Embassy in China for the funding of the joint French-Chinese PhD program. This work is supported by CNES (Centre National d'Etudes Spatiales) under contract No. RS06/SU-0002-041 and the NSFC under contracts No. 10673033 and No. 10621303.

REFERENCES

[1] J. Baubert, P. Khosropanah, V. Desmaris, V. Drakinskiy, P. Pons, P. Calmon, H. Merkel, M. Salez, "FTS measurement of a 2.5 THz double slot antenna on SiO_2/Si_3N_4 membrane with a NbN HEB mixer," in *Proc. 16th Int. Symp. Space Terahertz Technology,* 2005, pp. 260–264.

[2] D. F. Filipovic, S. S. Gearhart, and G. M. Rebeiz, "Double slot antennas on extended hemispherical and elliptical silicon dielectric lenses," *IEEE Trans. Microwave Theory Tech.,* vol. 41, pp. 1738-1749, 1993.

[3] G. V. Eleftheriades *et al.*, "Self and mutual admittance of slot antennas on a dielectric half space," *Int. J. Infrared Millimeter Waves,* vol. 14, pp. 1925–1946, 1993.

[4] *Computer Simulation Technology,* http://www.cst.com/

[5] *High Frequency Structure Simulator*, http://www.ansoft.com/.

[6] *Feldberechnung bei Korpern mit beliebieger Oberflache: Field computations involving bodies of arbitrary shape*, http://www.feko.info/.

[7] A. D. Semenov *et al.*, "Design and performance of the lattice-cooled hot-electron terahertz mixer," *Int. J. Applied Physics,* vol. 88, pp. 6758–6767, 2000.

[8] *RT/Duroid 6006/6010 LM High Frequency Laminates*, http://www.rogerscorporation.com/.

[9] W. Zhang, C. Y. Edward Tong, and S. C. Shi, "Scale model measurement of the embedding impedance of a 660-GHz waveguide SIS mixer with a 3-stardard de-embedding method," *IEEE Microwave and Wireless Component Letters,* vol. 13, no. 9, pp. 376–378, 2003.

[10] S. Ramo, J. R. Whinnery, and T. Van Duzer, *Fields and Waves in Communication Electronics*, 2nd ed. New York: Wiley, 1984, pp. 538.